Journal of Biomedical Optics

SPIEDigitalLibrary.org/jbo

Noninvasive three-dimensional live imaging methodology for the spindles at meiosis and mitosis

Jing-gao Zheng
Tiancheng Huo
Ning Tian
Tianyuan Chen
Chengming Wang
Ning Zhang
Fengying Zhao
Danyu Lu
Dieyan Chen
Wanyun Ma
Jia-lin Sun
Ping Xue

SPIE

Noninvasive three-dimensional live imaging methodology for the spindles at meiosis and mitosis

Jing-gao Zheng,[a] Tiancheng Huo,[a] Ning Tian,[a] Tianyuan Chen,[a] Chengming Wang,[a] Ning Zhang,[a] Fengying Zhao,[a] Danyu Lu,[b] Dieyan Chen,[a] Wanyun Ma,[a] Jia-lin Sun,[a] and Ping Xue[a]

[a]Tsinghua University, Department of Physics and State Key Lab of Low-Dimensional Quantum Physics, Beijing 100084, China
[b]Peking University, Department of Anatomy & Histology and Embryology, School of Basic Medical Sciences, Health Science Center, Beijing 100191, China

Abstract. The spindle plays a crucial role in normal chromosome alignment and segregation during meiosis and mitosis. Studying spindles in living cells noninvasively is of great value in assisted reproduction technology (ART). Here, we present a novel spindle imaging methodology, full-field optical coherence tomography (FF-OCT). Without any dye labeling and fixation, we demonstrate the first successful application of FF-OCT to noninvasive three-dimensional (3-D) live imaging of the meiotic spindles within the mouse living oocytes at metaphase II as well as the mitotic spindles in the living zygotes at metaphase and telophase. By post-processing of the 3-D dataset obtained with FF-OCT, the important morphological and spatial parameters of the spindles, such as short and long axes, spatial localization, and the angle of meiotic spindle deviation from the first polar body in the oocyte were precisely measured with the spatial resolution of 0.7 μm. Our results reveal the potential of FF-OCT as an imaging tool capable of noninvasive 3-D live morphological analysis for spindles, which might be useful to ART related procedures and many other spindle related studies. [DOI: 10.1117/1.JBO.18.5.050505]

Keywords: spindle; scattering; noninvasive; full-field optical coherence tomography.

Paper 130110LR received Feb. 28, 2013; revised manuscript received Apr. 15, 2013; accepted for publication Apr. 17, 2013; published online May 9, 2013.

The spindles are composed of microtubules and play key roles in proper chromosome alignment and segregation during meiosis and mitosis. Defects in either meiotic spindle of the oocyte or mitotic spindle of the zygote can cause chromosome misalignments, resulting in subsequent aneuploidy, infertility, spontaneous abortions, and congenital malformations.[1,2] To achieve embryos of better quality and higher pregnancy rate in assisted reproduction technology (ART), a great many groups made attempts for investigating the relationship between the presence/location/abnormalities of the spindles and various ART related outcomes.[3–5]

To visualize and evaluate the structures of spindles, a lot of spindle-imaging systems have been utilized and developed. Confocal microscopy and transmission electron microscopy can image the detailed structure of the spindles, but these methods use fixed or labeled samples, providing limited value for dynamic and subsequent developmental studies.[3] To image the spindles noninvasively, polarized light microscopy, which is based on the birefringence, is used. Nonetheless, orientation-dependent and nonquantitative characteristics limit its value in further analysis.[6] To meet the clinical and research need, the Polscope is developed.[7] With the Polscope, spindles can be visualized noninvasively regardless of their orientation. However, it has been reported that sometimes the spindles became visible only after manual rotation with micropipette even when using the Polscope.[8] Furthermore, because the Polscope measures the retardance, which is accumulative effect of optical property, it fails to achieve three-dimensional (3-D) morphology of the samples. Until now, a method that simultaneously allows noninvasive, perfectly orientation-independent, and 3-D imaging of the spindles in living cells has never been demonstrated.

Full-field optical coherence tomography (FF-OCT) is an attractive biomedical imaging technology, which has all these characteristics.[9,10] FF-OCT creates contrast on the basis of optical scattering property. By measuring the backscattered light from the sample, it performs optical slicing without any need of real excision, preprocessing, and staining, making noninvasive visualization and orientation-independent 3-D reconstruction possible. In contrast to confocal microscopy, FF-OCT illuminates the entire field of view uniformly, and hence its optical power density on the sample is 7 to 10 orders of magnitude lower.[11,12] By adapting the broadband light source and high N.A. microscope objectives, subcellular resolution can be achieved both in axial and transverse directions. For these reasons, FF-OCT has become a worthy imaging modality in developmental biology.[12–15] Recently, our group reported that the nucleus was successfully imaged with FF-OCT.[12,15] These studies indicated that as long as the scattering properties of other organelles differed from that of the cytoplasm, FF-OCT might also produce enough contrast to visualize these structures. However, its capabilities of imaging the spindles have never been examined so far.

In this paper, we demonstrate the first successful application of FF-OCT to noninvasive 3-D morphological imaging of the meiotic and mitotic spindles in living oocytes and zygotes. Also, by post-processing of the 3-D dataset obtained with FF-OCT, useful morphological and spatial parameters of the spindles are accurately quantified. Our studies suggest that the technique of FF-OCT is a powerful methodology for imaging the spindles and may be helpful to spindle related research.

The schematic of FF-OCT setup is shown in Fig. 1. It was based on the Linnik interference microscope geometry with a tungsten-halogen lamp, illuminating the entire sample field of view uniformly with the optical power density of 0.2 W/cm^2. The central wavelength of the light source was 600 nm, and the spectral bandwidth was 180 nm, corresponding to an

Address all correspondence to: Ping Xue and Jia-lin Sun, Tsinghua University, Department of Physics and State Key Lab of Low-Dimensional Quantum Physics, Haidian District, Beijing, 100084 China. Tel: +86-10-62784531-197 and 86-10-62772687; Fax: 86-10-62781598; E-mail: xuep@tsinghua.edu.cn and jlsun@tsinghua.edu.cn

axial resolution of 0.7 μm in water. Our FF-OCT employed two identical water-immersion microscope objectives (Nikon 20×, 0.5 N.A.) in both arms, achieving a transverse resolution of 0.7 μm. The interferograms resulted from the back-reflected light of both arms were digitized by a two-dimensional (2-D) silicon charge-coupled device camera array (IMPERX, MDC-1004, 48 Hz). A YAG crystal was placed in the reference arm and attached to a piezoelectric transducer (PZT). PZT was used to extract enface tomographic signals.[10] A motorized translation stage was placed in the sample arm, moving the sample in the axial (Z) direction to get a 3-D volumetric image. There was an incubator on the translation stage providing 37°C, 5% CO_2 to keep the embryos alive.

In our studies, wild-type ICR/CD1 mice (Laboratory Animal Facility, Tsinghua University, PRC) were used. To collect *in vivo* matured oocytes that arrested at the second meiotic metaphase (MII-arrested oocytes), females (eight-week-old) were superovulated by injecting 5 IU of pregnant mare's serum gonadotrophin (Bo'en Pharmaceutical Ltd., Chifeng, PRC). 48 h later, 5 IU of human chorionic gonadotropin (Livzon Pharmaceutical Group Inc., Zhuhai, PRC) was injected, and then the oocytes were obtained from the oviducts 17 h later. Cumulus cells were removed by brief incubation in 0.05% hyaluronidase (Sigma, Louis, MO; cat. no. H3506) at 37°C for 5 min. On the other hand, to collect zygotes at the mitotic metaphase and telophase, females were mated overnight with males and examined for vaginal plugs. The presence of a plug was taken as E0.5. The zygotes at the mitotic metaphase and telophase obtained at the period between late E0.5 and early E1.5. For live imaging, the oocytes and the zygotes were then immediately placed into a droplet of human tubal fluid (HTF) medium with 20% FBS (Hyclone, USA) covered with mineral oil (M4080, Sigma, USA) in our incubator. About 80 and 70 optical slices were needed to scan the entire oocytes and zygotes, respectively, using the axial step of 1.2 μm. The imaging rate was 1.25 s per optical slice.

The MII-arrested oocyte has two notable morphological characteristics. One is that the meiotic spindle appears in the outermost layer of the cytoplasm of the oocyte and orients with its long axis parallel to the cortical membrane. The other one is that the chromosomes are controlled by the spindle and aligned in the mid-region of the spindle. Figure 2(a) shows the 3-D cross-section view of a typical MII-arrested oocyte with FF-OCT. Besides zona pellucida (ZP), the first polar body (1PB) and the cytoplasm of the oocyte, a relatively dark and long area, which extends along the cortical membrane, is also visible with enough contrast against the oocyte cytoplasm. To see the area more clearly, image cropping and color inversion were applied to the 3-D dataset obtained with FF-OCT. Figure 2(b) shows the 3-D reconstruction of this dark area after these image processings. Therefore, the cropped dark area appears bright in the figure. By the shape and orientation, the area was ascertained to be the spindle. To confirm this further, we employed the immunofluorescence technique to label the spindle (SP) and chromosomes (CH) of the same oocyte and scanned it with two-photon laser scanning microscopy (TPLSM). Figure 2(c) shows the false-color 3-D reconstruction of the Quantum dot 585-labeled spindle and Hoechst 33342-stained chromosomes. Detailed structures of the spindle can be seen, and the chromosomes in the mid-region are clearly visible as well. Then, using the 3-D dataset obtained with FF-OCT and TPLSM, we measured the short and long axes of the bright area in Fig. 2(b) and the spindle in Fig. 2(c). As a result, the lengths of short and long axes were 11.7 and 26.6 μm with TPLSM. While with FF-OCT, the lengths were 11.2 and 27.0 μm, consistent with the TPLSM's measurements with the accuracy of FF-OCT resolution. Therefore, we affirm that the dark area in the FF-OCT images is the spindle, reflecting the microtubules of the spindle are of lower scattering coefficient than the cytoplasm. On the

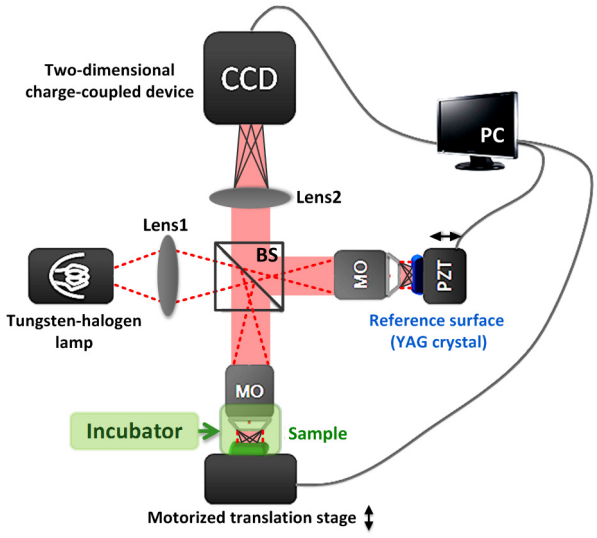

Fig. 1 Schematic diagram of FF-OCT based on the Linnik interference microscope. BS, beam splitter; MO, microscope objectives; PZT, piezoelectric transducer; PC, personal computer.

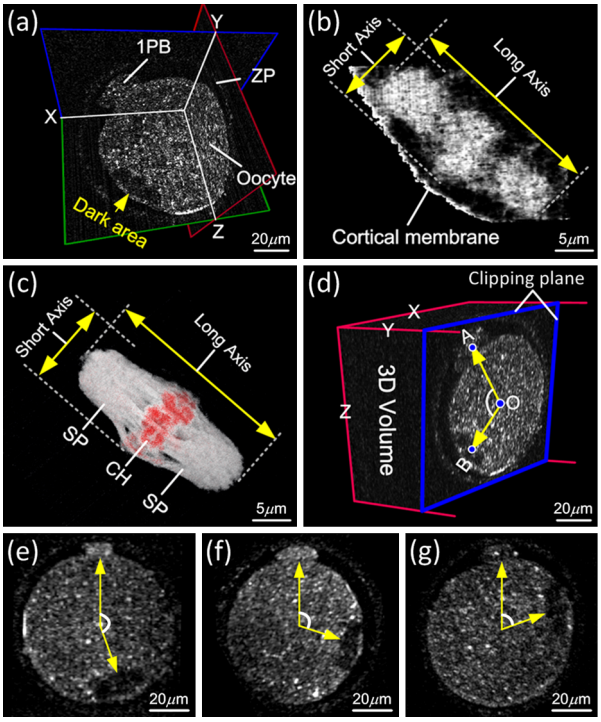

Fig. 2 (a) 3-D cross-section view of a typical MII-arrested oocyte using FF-OCT; (b) 3-D reconstruction of the dark area in (a) after cropping and color inversion; (c) 3-D reconstructions of the spindle and the chromosomes of the same oocyte using TPLSM; (d) A cross-section view where the centers of the oocyte, 1PB and the spindle can be seen at the same time using 3-D dataset obtained with FF-OCT; (e)–(g) Other oocytes with different angles of meiotic spindle deviation from the 1PB.

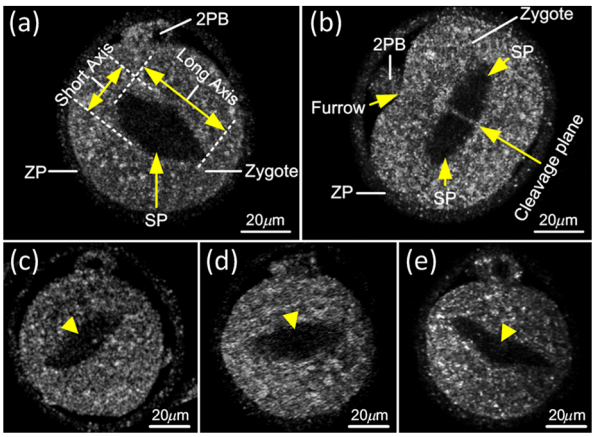

Fig. 3 Mitotic spindle imaging of the zygotes (a) at metaphase and (b) at telophase. (c)–(e) Other zygotes with mitotic spindles (arrow).

other hand, because the nucleus was less scattering than the cytoplasm,[12] the chromosomes that aligned in the metaphase plate also contributed to the low brightness of the mid-region of the spindle in Fig. 2(a).

In addition, when using the Polscope, to measure the angle of meiotic spindle deviation from the 1PB, the oocyte has to be manually rotated, not only until both of the 1PB and the spindle can be clearly viewed in the same observation plane, but also until the spindle appears in the outermost layer of the cytoplasm. However, no matter how the 1PB and the spindle orient, just by post-processing, the angle can be precisely measured using the 3-D dataset obtained with FF-OCT. To measure the angle, 3-D geometry centers of the cytoplasm, the 1PB, and the spindle of the oocyte were calculated. Point O, A, and B in Fig. 2(d) are the corresponding 3-D geometry centers. With these three centers, the angle was quantified to be 101 deg. On the other hand, because the 1PB and the spindle were not oriented in the same XY plane as shown in Fig. 2(a), when scanning in the Z direction with FF-OCT, the two structures cannot appear in the same observation plane. However, by clipping the 3-D volume of the oocyte with a plane, which contains these three points, the 1PB and the spindle can also be simultaneously seen in a cross-section view, as shown in Fig. 2(d). Figures 2(e) to 2(g) show other oocytes with different angles of meiotic spindle deviation from the 1PB. The angles were measured to be 160, 108, and 70 deg, respectively. Accurate measurement of the angle in this way avoids the subjectivities of observers and is more reliable. Therefore, FF-OCT may provide new insight into the relationship between the angle and subsequent developmental competence.

Also, to demonstrate the capabilities of FF-OCT to image the mitotic spindle, the zygotes at the metaphase and telophase were imaged. Figure 3(a) shows the cross-section view of a typical zygote at metaphase. In Fig. 3(a), the spindle can be clearly seen in the middle of the zygote. The short and long axes of this spindle were quantified to be 23.9 and 43.2 μm, respectively. Figure 3(b) shows the cross-section view of a typical zygote at telophase. In Fig. 3(b), the spindle has been divided into two parts, and the cleavage furrow has been established. The bright area between the separated spindles would be the first cleavage plane of the zygote. The interesting structures of the spindles both in Fig. 3(a) and 3(b) obtained by FF-OCT were in good accord with the biological characteristics at mitotic metaphase and telophase. Figures 3(c) to 3(e) show other zygotes with mitotic spindles (arrow). Therefore, with FF-OCT, 3-D morphological images of the spindles can be achieved in living cells without any fixation and staining both at meiosis and mitosis.

In conclusion, we presented FF-OCT as a novel technique for viewing the meiotic and mitotic spindles in the living cells with no need of preprocessing and labeling. Using 3-D optical slices obtained with FF-OCT, the morphological and spatial parameters of the spindles were precisely measured with the spatial resolution of 0.7 μm. Our results suggested that FF-OCT might be valuable in ART and many other spindle related studies.

Acknowledgments

This work was sponsored in part by the Ministry of Science and Technology of China contracts 2006AA02Z472, 2007CB511904, 001CB510307, and 2009CB929400 by the National Natural Science Foundation of China Grant 61227807, and by the Ministry of Education of China Grant 20130002110079 for Doctoral Program.

References

1. E. Mantikou et al., "Molecular origin of mitotic aneuploidies in preimplantation embryos," *Biochim. Biophys. Acta* **1822**(12), 1921–1930 (2012).
2. U. Eichenlaub-Ritter et al., "Manipulation of the oocyte: possible damage to the spindle apparatus," *Reprod. Biomed. Online* **5**(2), 117–124 (2002).
3. A. Borini et al., "Predictive factors for embryo implantation potential," *Reprod. Biomed. Online* **10**(5), 653–668 (2005).
4. C. G. Petersen et al., "Relationship between visualization of meiotic spindle in human oocytes and ICSI outcomes: a meta-analysis," *Reprod. Biomed. Online* **18**(2), 235–243 (2009).
5. Y. F. Gu et al., "Analysis of the first mitotic spindles in human in vitro fertilized tripronuclear zygotes after pronuclear removal," *Reprod. Biomed. Online* **19**(5), 745–754 (2009).
6. R. Oldenbourg, "Polarized light microscopy of spindles," *Method. Cell. Biol.* **61**, 175–208 (1999).
7. L. Liu et al., "A reliable, noninvasive technique for spindle imaging and enucleation of mammalian oocytes," *Nat. Biotechnol.* **18**(2), 223–225 (2000).
8. L. Rienzi et al., "Relationship between meiotic spindle location with regard to the polar body position and oocyte developmental potential after ICSI," *Hum. Reprod.* **18**(6), 1289–1293 (2003).
9. A. Dubois et al., "Ultrahigh-resolution full-field optical coherence tomography," *Appl. Opt.* **43**(14), 2874–2883 (2004).
10. D. Sacchet et al., "Simultaneous dual-band ultra-high resolution full-field optical coherence tomography," *Opt. Express* **16**(24), 19434–19446 (2008).
11. M. Göppert-Mayer, "Über Elementarakte mit zwei Quantensprüngen," *Ann. Phys.* **401**(3), 273–294 (1931).
12. J. G. Zheng et al., "Label-free subcellular 3D live imaging of preimplantation mouse embryos with full-field optical coherence tomography," *J. Biomed. Opt.* **17**(7), 070503 (2012).
13. W. Y. Oh et al., "Ultrahigh-resolution full-field optical coherence microscopy using InGaAs camera," *Opt. Express* **14**(2), 726–735 (2006).
14. A. Perea-Gomez et al., "Initiation of gastrulation in the mouse embryo is preceded by an apparent shift in the orientation of the anterior-posterior axis," *Curr. Biol.* **14**(3), 197–207 (2004).
15. J. G. Zheng et al., "Understanding three-dimensional spatial relationship between the mouse second polar body and first cleavage plane with full-field optical coherence tomography," *J. Biomed. Opt.* **18**(1), 010503 (2013).